Bilayer effects on the electronic spectra of doped cuprates

Amit Pratap,[1] Ratan Lal,[1] Govind,[1] and S. K. Joshi[1,2]
[1]*Theory Group, National Physical Laboratory, New Delhi-110012, India*
[2]*Jawaharlal Nehru Centre for Advanced Scientific Research, Jakkur, Bangalore-560064, India*
(Received 17 May 2001; published 21 November 2001)

A self-consistent perturbative approach has been used for investigating the effects of bilayer coupling in cuprate systems possessing two CuO_2 layers per unit cell. The strong electron correlation effects which exist in the individual CuO_2 layers are described by a t-t'-J model, and the coupling between the two intraunit cell layers is included via a layer-to-layer hopping matrix element $t_\perp$ and an exchange interaction $J_\perp$. Calculations of the electronic spectral function $A(\mathbf{k},\omega)$ have been made for different values of the hole concentration, temperature, and anisotropy for analyzing the appropriate conditions for the splitting of the quasiparticle peak in the normal state. It has been found that the splitting of the quasiparticle peak becomes favorable for higher values of the hole doping and higher anisotropy ratios. Calculations of the imaginary part of the self-energy $\Sigma_1''(\mathbf{k},\omega)$ have also been made. It has been found that $\Sigma_1''(\mathbf{k},\omega)$ depends strongly on the momentum $\mathbf{k}$ and that the energy dependence of $\Sigma_1''(\mathbf{k},\omega)$ changes qualitatively with the change of the momentum $\mathbf{k}$. For $\mathbf{k}=(0,0)$ a Fermi liquid like behavior is found for low ω, while for other values of momentum, considered here, $\Sigma_1''(\mathbf{k},\omega)$ varies like $\omega^\alpha(1<\alpha<2)$.

DOI: 10.1103/PhysRevB.64.224512 PACS number(s): 74.25.Jb, 74.72.Bk, 74.72.Hs

I. INTRODUCTION

Cuprates like La_2CuO_4, $YBa_2Cu_3O_6$, and $Bi_2Sr_2CaCu_2O_8$ have one hole on each Cu atom.[1] The spins of these holes interact via a superexchange interaction, leading to an antiferromagnetic insulating state.[2] When these systems are doped with holes either by partially substituting a trivalent atom by a divalent one, or by changing the oxygen content, the antiferromagnetic long-range order starts to weaken rapidly.[3] With an increase in the density of doped holes (δ) a stage occurs when the long-range antiferromagnetic order is completely destroyed and the system tends to enter a metallic phase with short-range spin correlations.[4] On lowering the temperature of the metallic system below a critical value (T_c), it switches to a superconducting state. Metallic as well as superconducting states can be probed by angle-resolved photoemission spectroscopy (ARPES) which has proved itself to be an excellent tool in gaining information about the response function of the doped holes.[5] In 1990 Olson *et al.*[6] measured the ARPES spectrum of $Bi_2Sr_2CaCu_2O_{8+y}$ samples which seemed to show a dip in the spectral weight at $\sim$90 meV along the Γ-$\bar{M}$ $\mathbf{k}$-space direction in the superconducting state. Later, Dessau *et al.*[7] obtained the temperature-dependent ARPES spectrum of $Bi_2Sr_2CaCu_2O_{8+y}$, and reported a dip at $\sim$90 meV along the Γ-$\bar{M}$ $\mathbf{k}$-space direction when the system is cooled below its superconducting transition temperature. On the other hand, no dip was observed along the Γ-X $\mathbf{k}$-space direction.[7] Recent ARPES measurements showed, the effect of a dip in the form of splitting in the electronic states of an overdoped bilayer system ($Bi_2Sr_2CaCu_2O_{8+y}$) near the Fermi energy in the normal state ($T=90\,\mathrm{K}>T_c=65\,\mathrm{K}$ (Ref. 8) and $T=100\,\mathrm{K}>T_c=85\,\mathrm{K}$ (Ref. 9). The splitting is observed to vanish along the Γ-X nodal line in reciprocal space, and is seen to be maximum at the k point $(\pi,0)$. However, such a splitting has not been observed in compounds like $La_{2-x}Sr_xCuO_4$ and $Bi_2Sr_2CuO_{6+\delta}$, which have only one CuO_2 layer per unit cell.[5,8–10] This is a clear indication of the importance of coupling between the two CuO_2 planes in the same unit cell and its association with the splitting of electronic states. On the other hand, it is also observed that the peak splitting does not appear in the underdoped bilayer cuprates.[11]

Theoretical studies of spectral properties have so far been limited mainly to single, layer systems like $La_{2-x}Sr_xCuO_4$.[12–24] Moreover, most of these studies were confined to one (or two) hole(s) added to the antiferromagnetic background formed by a cluster of few sites. The main methods used so far for the study of spectral properties of cuprates included the exact diagonalization method.[13–15] The quantum Monte Carlo method,[16–19] the density-matrix renormalization group method[20,21] and the finite-temperature Lanczos method (FTLM).[22–24] The FTLM was also used to study the dynamics of overdoped cuprates.[24] Compared to the vast theoretical studies of the single-layer cuprates,[12–24] there are only a few theoretical studies of the bilayer cuprates.[25,26]

In this paper we study the spectral properties of bilayer cuprates for various values of doping, temperature and the strength of intrabilayer interactions. We shall, in particular, address the question why splitting is not observed in underdoped samples. In order to understand the role of bilayer coupling in the dynamics of cuprates, we consider a system like $YBa_2Cu_3O_{7-y}$ or $Bi_2Sr_2CaCu_2O_{8+y}$ having two CuO_2 layers per unit cell. We calculated the spectral function $A(\mathbf{k},\omega)$ and the imaginary part of the self energy $\Sigma_1''(\mathbf{k},\omega)$ for different values of doping and temperature for these bilayer systems. For this, we describe the individual layers by a t-t'-J model and couple these layers via a hopping process of holes as well as an exchange coupling between the spins in these layers. We apply an equation-of-motion method and obtain an expression of the Green's function $G(\mathbf{k},\omega)$ for the holes within a self-consistent perturbative approach. Expres-

sion for the self-energy is obtained by solving the Dyson equation within the first Born approximation. Details of our theoretical calculations are described in Sec. II. Numerical calculations and results of the spectral function and the imaginary part of the self energy are presented in Sec. III. The results for spectral functions and the imaginary part of the self-energy are discussed in the light of recent ARPES measurements.

II. THEORETICAL FORMULATION

In bilayer cuprate systems like $YBa_2Cu_3O_{7-y}$ and $Bi_2Sr_2CaCu_2O_{8+y}$, the two CuO_2 layers in the same unit cell are relatively closer ($d_1 \sim 0.4$ nm) than the CuO_2 layers of the two neighboring unit cells ($d_2 \sim 0.7$ nm). In fact d_1 is comparable to the intralayer Cu-Cu distance. It was confirmed by neutron-scattering experiments that the spins of the two layers in the same unit cell are coupled antiferromagnetically, so that the signatures of such coupling should appear in the doped and the superconducting phases of these systems.[27,28]

We assume that each layer of the bilayer cuprates is described by the t-t'-J model:

$$\mathbf{H}^1_{t-J} = \sum_{ij\sigma} t_{ij} \mathbf{1}^+_{i\sigma} \mathbf{1}_{j\sigma} + J_{\parallel} \sum_{ij} \mathbf{S}_{il} \cdot \mathbf{S}_{jl}. \tag{1}$$

Here $l=1$ and 2 denote the two CuO_2 layers of the unit cell, and t_{ij} is the hopping matrix element for hopping of a hole from site i to site j within the layers. In the present paper, in addition to the nearest-neighbor hopping ($t_{\parallel}$), we have also considered the next-nearest-neighbor hopping (t') within the two-dimensional CuO_2 plane. $l^+_{i\sigma}(l_{i\sigma})$ is the creation (annihilation) operator of the correlated hole of spin σ at site i. These operators are related with the uncorrelated creation (annihilation) operators $l^+_{0i\sigma}(l_{0i\sigma})$ by

$$l^+_{i\sigma} = l^+_{0i\sigma}(1 - l^+_{0i-\sigma} l_{0i-\sigma}) \tag{2}$$

and

$$l_{i\sigma} = (1 - l^+_{0i-\sigma} l_{0i-\sigma}) l_{0i\sigma}. \tag{3}$$

In Eq. (1), S_{il} is spin operator at the ith site of layer l. $J_{\parallel}$ is the exchange coupling strength between the nearest-neighbor spins in the same CuO_2 plane. For a bilayer cuprate when we consider the coupling between the two layers in the same unit cell, the total Hamiltonian would be

$$H = H^1_{t-J} + H^2_{t-J} + H'_{t_\perp} + H'_{J_\perp}, \tag{4}$$

where $H'_{t_\perp}$ corresponds to the hopping between the two layers within the unit cell, and $H'_{J_\perp}$ corresponds to the exchange coupling between these two layers. For a clear distinction between layer 1 and layer 2, we write $1^{(+)}_{i\sigma} = c^{(+)}_{1i\sigma}$ for layer $l=1$ and $1^{(+)}_{i\sigma} = c^{(+)}_{2i\sigma}$ for layer $l=2$. In this notation the Hamiltonian would read

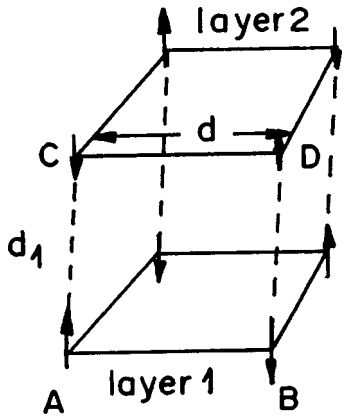

FIG. 1. Schematic representation of the unit cell of a bilayer cuprate showing the four sublattices (*A, B, C,* and *D*) having spins up and down at Cu sites.

$$H = \sum_{ijl\sigma} t_{ij} c^+_{li\sigma} c_{lj\sigma} + \sum_{l\neq l' i\sigma} t_\perp c^+_{li\sigma} c_{l'i\sigma} + J_{\parallel} \sum_{ijl} S_{il} . S_{jl} + J_\perp \sum_{l\neq l' i} S_{il} . S_{il'}. \tag{5}$$

Here $t_\perp$ is the hopping matrix element for hopping of holes between the two layers in the cell, and $J_\perp$ is the exchange coupling strength between the spins of two layers l and l' in the same unit cell.

In order to derive the spectral function $A(\mathbf{k},\omega)$ and the imaginary part of the self-energy $\Sigma''(\mathbf{k},\omega)$ for Hamiltonian (5), we employ a self-consistent perturbative approach by considering the magnetic interactions in terms of a ferromagnetic background as suggested in Ref. 29. In fact, the ground state of the bilayer cuprates is a Neel antiferromagnet which may be considered as composed of four sublattices having spins say up at A (layer 1) and D (layer 2) sublattices, and spin-down at B (layer 1) and C (layer 2) sublattices, as shown in Fig. 1. For the down spins of sublattices B and C, we perform a spin-down to spin-up transformation, so that all the four sublattices then have their spins pointing upward. When site i belongs to sublattice B or C, the spin down to spin up transformation will be

$$c_{1i\sigma}(c_{2i\sigma}) = c_{1i-\sigma}(c_{2i-\sigma}), \quad S^{\pm}_{il} = S^{\mp}_{il}; S^z_{il} = -S^z_{il}.$$

In order to handle the spin operators in a practical way, we consider the hole operator ($c_{li\sigma}$) in the form of the product of two parts—one having charge only and the other representing the spin character. Let $f^+_{li}(f_{li})$ denote the creation (annihilation) operator corresponding to the spinless fermions, and s_{li} be the pseudospin operator in the lth layer at site i Then the hole operators may be written as[29]

$$c_{li\uparrow} = f^+_{li} \pi_{li}, \tag{6a}$$

$$c_{li\downarrow} = f^+_{li} s^+_{li}, \tag{6b}$$

and

$$\mathbf{S}_{li} = \mathbf{s}_{li}(1 - n_{li}) \tag{6c}$$

where $n_{li}=f_{li}^{+}f_{li}$ denotes the number of the spinless fermions operator at site i of layer 1, π_{li} denotes the projection operators to eliminate the unphysical states, and this gives[29]

$$\pi_{li}=\tfrac{1}{2}+s_{li}^{z}, \tag{7}$$

$$\pi_{li}\left|\tfrac{1}{2}\right\rangle=1. \tag{8}$$

One of the effects of the transformation given by Eq. (6) is that it modifies the exchange term by a factor $(1-\delta)^2$. This means that the $J_{\parallel}$ and $J_{\perp}$ will be replaced by the new parameters $\tilde{J}_{\parallel}=J_{\parallel}(1-\delta)^2$ and $\tilde{J}_{\perp}=J_{\perp}(1-\delta)^2$, respectively. We apply transformations (6) to the terms of Hamiltonian (5), and write the transformed Hamiltonian in the k representation:

$$\begin{aligned}H=&\sum_{kq}\{t(k-q)f_{1k-q}f_{1k}^{+}s_{1q}^{+}+t(k)f_{1k+q}f_{1k}^{+}s_{1q}^{-}\}\\&+\sum_{kq}\{t(k-q)f_{2k-q}f_{2k}^{+}s_{2q}^{+}+t(k)f_{2k+q}f_{2k}^{+}s_{2q}^{-}\}\\&+\sum_{kq}\{t_{\perp}(k-q)f_{1k-q}f_{2k}^{+}s_{2q}^{+}+t_{\perp}(k)f_{1k+q}f_{2k}^{+}s_{1q}^{-}\}\\&+\sum_{lq}J_{\parallel}(q)\{s_{lq}^{+}s_{l-q}^{+}+s_{lq}^{-}s_{l-q}^{-}\}-\sum_{lq}2z_{ab}\tilde{J}_{\parallel}\{s_{lq}^{z}s_{l-q}^{z}\}\\&+\sum_{l\neq l'q}\tilde{J}_{\perp}\{s_{lq}^{+}s_{l'-q}^{+}+s_{lq}^{-}s_{l'\beta-q}^{-}\}-\sum_{l\neq l'q}2\tilde{J}_{\perp}\{s_{lq}^{z}s_{l'-q}^{z}\},\end{aligned} \tag{9}$$

where

$$t(k)=-2st_{\parallel}(\cos k_x+\cos k_y)-4t'\cos k_x\cos k_y, \tag{10}$$

$$J_{\parallel}(q)=2sz_{ab}\tilde{J}_{\parallel}(\cos q_x+\cos q_y), \tag{11}$$

where $z_{ab}(=4)$ is the number of nearest neighbors within the two-dimensional lattice of the CuO_2 plane. $t_{\parallel}$ is the bare hole hopping to the nearest-neighbor sites in a layer, and t' is the hopping to the next-nearest-neighbor sites of the same layer. In Eqs. (10) and (11), we take the in-plane lattice constant $a=1$.

In Eq. (9) $t_{\perp}(k)$ is the hopping matrix element of a hole from one layer to the another layer. In the literature, $t_{\perp}(k)$ has been considered to be dependent on k_x and k_y such that

$$t_{\perp}(k)=t_{\perp}(\cos k_x-\cos k_y)^2 \tag{12}$$

In fact, Eq. (12) is based on the experimental fact that there is no hopping of holes between the two layers along the $k_x=k_y$ direction.

We now define the following Green's functions corresponding to the spinless fermions.

$$G_{kk'}(\omega)=\langle\langle f_{1k}|f_{1k'}^{+}\rangle\rangle \text{ and } F_{kk'}(\omega)=\langle\langle f_{2k}|f_{1k'}^{+}\rangle\rangle. \tag{13}$$

Here ω denotes the energy, $G_{kk'}(\omega)$ corresponds to the motion of spinless fermions in the same layer, and $F_{kk'}(\omega)$ corresponds to that from one layer to the another layer. Writing the equations of motion for the Green's functions $G_{kk'}(\omega)$ and $F_{kk'}(\omega)$ we encounter the usual irreducible part of the Green's function. The irreducible part has been evaluated by restricting ourselves to the first Born approximation. In this manner we obtain

$$\left(\omega-\sum_{1}\right)G_{kk'}=\frac{1}{2\pi}+\sum_{2}F_{kk'} \tag{14}$$

and

$$\left(\omega-\sum_{1}\right)F_{kk'}=\sum_{2}G_{kk'}. \tag{15}$$

For the sake of abridging the expressions, the $\mathbf{k}$ and ω dependences of self-energies $\Sigma_1(\mathbf{k},\omega)$ and $\Sigma_2(\mathbf{k},\omega)$, as well as the vector representations of $\mathbf{k}$ and $\mathbf{q}$ in the argument, are not shown in the expressions. The expressions for Σ_1 and Σ_2 are given by

$$\begin{aligned}\sum_{1}=&\frac{1}{2s}\sum_{q}[t(k-q)t(k-q)\langle s_{1q}^{-}s_{1q}^{+}\rangle+t(k-q)t(k)\langle s_{1-q}^{+}s_{1q}^{+}\rangle]D_1+[t(k)t(k-q)\langle s_{1q}^{-}s_{1-q}^{-}\rangle+t(k)t(k)\langle s_{1-q}^{+}s_{1-q}^{-}\rangle]D_2\\&+[t_{\perp}(k)t(k-q)\langle s_{1q}^{-}s_{2-q}^{-}\rangle+t_{\perp}(k)t(k)\langle s_{1-q}^{+}s_{2-q}^{-}\rangle]D_3+[t_{\perp}(k-q)t(k-q)\langle s_{1q}^{-}s_{2q}^{+}\rangle+t_{\perp}(k-q)t(k)\langle s_{1-q}^{+}s_{2q}^{+}\rangle]D_4\end{aligned} \tag{16}$$

and

$$\begin{aligned}\sum_{2}=&\frac{1}{2s}\sum_{q}[t(k-q)t_{\perp}(k-q)\langle s_{2q}^{-}s_{1q}^{+}\rangle+t(k-q)t_{\perp}(k)\langle s_{1-q}^{+}s_{1q}^{+}\rangle]D_1+[t(k)t_{\perp}(k-q)\langle s_{2q}^{-}s_{1-q}^{-}\rangle+t(k)t_{\perp}(k)\langle s_{1-q}^{+}s_{1-q}^{-}\rangle]D_2\\&+[t_{\perp}(k)t_{\perp}(k-q)\langle s_{2q}^{-}s_{2-q}^{-}\rangle+t_{\perp}(k)t_{\perp}(k)\langle s_{1-q}^{+}s_{2-q}^{-}\rangle]D_3+[t_{\perp}(k-q)t_{\perp}(k-q)\langle s_{2q}^{-}s_{2q}^{+}\rangle+t_{\perp}(k-q)t_{\perp}(k)\langle s_{1-q}^{+}s_{2q}^{+}\rangle]D_4.\end{aligned} \tag{17}$$

In Eqs. (16) and (17), the D_i's are Green's functions, corresponding to the pseudospin operators, which are defined as

$$D_q=\begin{bmatrix} D_1 \\ D_2 \\ D_3 \\ D_4 \end{bmatrix}=\begin{bmatrix} \langle\langle s^+_{1q}|s^-_{1q}\rangle\rangle \\ \langle\langle s^-_{1q}|s^-_{1q}\rangle\rangle \\ \langle\langle s^-_{2q}|s^-_{1q}\rangle\rangle \\ \langle\langle s^+_{2q}|s^-_{1q}\rangle\rangle \end{bmatrix}. \tag{18}$$

We emphasise that D_i's depend on the energy through ω, and are given explicitly by the expressions

$$D_1=s\left[\frac{\omega+J(0)-\lambda_1}{(\omega-\omega_1)(\omega-\omega_2)}+\frac{\omega+J(0)-\lambda_2}{(\omega-\omega_3)(\omega-\omega_4)}\right], \tag{19}$$

$$D_2=-s\left[\frac{J_\parallel(q)+4sJ_\perp-\lambda_3}{(\omega-\omega_1)(\omega-\omega_2)}+\frac{J_\parallel(q)-4sJ_\perp-\lambda_4}{(\omega-\omega_3)(\omega-\omega_4)}\right], \tag{20}$$

$$D_3=-s\left[\frac{J_\parallel(q)+4sJ_\perp-\lambda_3}{(\omega-\omega_1)(\omega-\omega_2)}-\frac{J_\parallel(q)-4sJ_\perp-\lambda_4}{(\omega-\omega_3)(\omega-\omega_4)}\right], \tag{21}$$

$$D_4=s\left[\frac{\omega+J(0)-\lambda_1}{(\omega-\omega_1)(\omega-\omega_2)}-\frac{\omega+J(0)-\lambda_2}{(\omega-\omega_3)(\omega-\omega_4)}\right]. \tag{22}$$

Here

$$\omega_{1,2}=\lambda_1\pm\sqrt{\omega^2_{1q0}+\lambda^2_3}, \tag{23}$$

$$\omega_{3,4}=\lambda_2\pm\sqrt{\omega^2_{2q0}+\lambda^2_4} \tag{24}$$

correspond to the magnon dispersion, and $\omega_{1,2q0}$ are given by

$$\omega_{1,2q0}=\sqrt{J^2(0)-\{J_\parallel(q)\pm 4s\tilde{J}_\perp\}^2} \tag{25}$$

and

$$J(0)=4z_{ab}s\tilde{J}_\parallel+4s\tilde{J}_\perp.$$

In Eqs. (24) and (25), λ_i's are the self-energy components, and are given by

$$\lambda_1=\eta_1(q,\omega)+\eta_4(q,\omega),\quad \lambda_2=\eta_1(q,\omega)-\eta_4(q,\omega),$$
$$\lambda_3=\eta_2(q,\omega)+\eta_3(q,\omega),\quad \lambda_4=\eta_2(q,\omega)-\eta_3(q,\omega) \tag{26}$$

with

$$\begin{aligned}\eta_1(q,\omega)=(2s)^2\sum_{kk'}\ &[t(k)t(k'-q)\langle\langle f_{1k+q}f^+_{1k}|f_{1k'-q}f^+_{1k'}\rangle\rangle \\ &+t(k)t_\perp(k')\langle\langle f_{1k+q}f^+_{1k}|f_{2k'}f^+_{1k'+q}\rangle\rangle] \\ &+[t_\perp(k)t(k'-q)\langle\langle f_{1k+q}f^+_{2k}|f_{1k'-q}f^+_{1k'}\rangle\rangle \\ &+t_\perp(k)t_\perp(k')\langle\langle f_{1k+q}f^+_{2k}|f_{2k'}f^+_{1k'+q}\rangle\rangle],\end{aligned} \tag{27}$$

$$\begin{aligned}\eta_2(q,\omega)=-(2s)^2\sum_{kk'}\ &[t(k-q)t(k'-q) \\ &\times\langle\langle f_{1k-q}f^+_{1k}|f_{1k'-q}f^+_{1k'}\rangle\rangle \\ &+t(k-q)t_\perp(k')\langle\langle f_{1k-q}f^-_{1k}|f_{2k'}f^-_{1k'-q}\rangle\rangle] \\ &+[t_\perp(k)t(k'-q)\langle\langle f_{2k}f^+_{1k+q}|f_{1k'-q}f^+_{1k'}\rangle\rangle \\ &+t_\perp(k)t_\perp\langle\langle f_{2k}f^+_{1k+q}|f_{2k'}f^-_{1k'+q}\rangle\rangle],\end{aligned} \tag{28}$$

$$\begin{aligned}\eta_3(q,\omega)=-(2s)^2\sum_{kk'}\ &[t(k-q)t(k'-q) \\ &\times\langle\langle f_{2k-q}f^+_{2k}|f_{1k'-q}f^+_{1k'}\rangle\rangle \\ &+t(k-q)t_\perp(k')\langle\langle f_{2k-q}f^-_{2k}|f_{2k'}f^-_{1k'-q}\rangle\rangle] \\ &+[t_\perp(k-q)t(k'-q)\langle\langle f_{1k-q}f^+_{2k}|f_{1k'-q}f^+_{1k'}\rangle\rangle \\ &+t_\perp(k-q)t_\perp(k')\langle\langle f_{1k-q}f^+_{2k}|f_{2k'}f^+_{1k'+q}\rangle\rangle],\end{aligned} \tag{29}$$

$$\begin{aligned}\eta_4(q,\omega)=(2s)^2\sum_{kk'}\ &[t(k)t(k'-q)\langle\langle f_{2k+q}f^+_{2k}|f_{1k'-q}f^+_{1k'}\rangle\rangle \\ &+t(k)t_\perp(k')\langle\langle f_{2k+q}f^+_{2k}|f_{2k'}f^+_{1k'-q}\rangle\rangle] \\ &+[t_\perp(k-q)t(k'-q)\langle\langle f_{2k}f^+_{1k-q}|f_{1k'-q}f^+_{1k'}\rangle\rangle \\ &+t_\perp(k-q)t_\perp(k')\langle\langle f_{2k}f^+_{1k-q}|f_{2k'}f^+_{1k'-q}\rangle\rangle].\end{aligned} \tag{30}$$

It is important to note that in the absence of doped holes, the system is an antiferromagnetic insulator. In this case the first two terms in the Hamiltonian of Eq. (5) vanish for the undoped system and the remaining part is just equivalent to the Heisenberg Hamiltonian for a bilayer system. The magnetic dynamics of such an undoped case studied earlier[27] suggests the existence of acoustic and optic branches as well as an optical magnon gap (at $\mathbf{q}=0$) in the magnon spectrum. We find that, in the absence of doped holes, $\delta=0$, and all λ's present in Eqs. (23) and (24) vanish and we retrieve the results for the undoped case.

Equations (27)–(30) involve the Green's functions of the product of four fermion operators. We obtain expressions for these Green's functions in a way discussed by Richard and Yushankhai.[29] We obtain

$$\langle\langle f_{1k+q}f^+_{1k}|f_{1k'-q}f^+_{1k'}\rangle\rangle=\left[\frac{n(\varepsilon_{k-q})-n(\varepsilon_k)}{(\omega+\varepsilon_{k-q}-\varepsilon_k+i0)}\right] \tag{31}$$

and

$$\langle\langle f_{1k+q} f^{+}_{2k} | f_{1k'-q} f^{+}_{1k'} \rangle\rangle$$
$$= \sum_{2} \left[\frac{n(\Sigma_1)}{(\Sigma_1 - \varepsilon_k)(\Sigma_1 - \omega - \varepsilon_{k-q})} + \frac{n(\varepsilon_k)}{(\varepsilon_k - \Sigma_1)(\varepsilon_k - \omega - \varepsilon_{k-q})} + \frac{n(\varepsilon_{k-q})}{(\omega + \varepsilon_{k-q} - \Sigma_1)(\omega + \varepsilon_{k-q} - \varepsilon_k)} \right]. \quad (32)$$

It is important to note that the term $\langle\langle f_{2k+q} f^{+}_{2k} | f_{1k'-q} f^{+}_{1k'} \rangle\rangle$ is proportional to $t_\perp^2$. Since $t_\perp \ll t_\parallel$ this Green's function is not expected to make a significant contribution to the dynamics of the system. We therefore neglect this term.

In Eqs. (31) and (32), $n(\varepsilon)$ is the Fermi function, and

$$\varepsilon_k = -2t_\parallel(\cos k_x + \cos k_y) - 4t' \cos k_x \cos k_y \quad (33)$$

is the bare hole dispersion. So far we have obtained the equations of motion for the hole Green's functions and spin Green's functions, and the expressions for various self-energy components λ_i. The spectral function $A(\mathbf{k},\omega)$ may now be evaluated by calculating the imaginary part of $G(\mathbf{k},\omega)$. In fact $G(\mathbf{k},\omega)$ is obtained by solving Eqs. (14) and (15). We obtain

$$G(\mathbf{k},\omega) = \frac{1}{[\omega - \Sigma(\mathbf{k},\omega)]}, \quad (34)$$

with

$$\sum (\mathbf{k},\omega) = \sum_{1} (\mathbf{k},\omega) + \frac{\Sigma_2^2(\mathbf{k},\omega)}{[\omega - \Sigma_1(\mathbf{k},\omega)]}. \quad (35)$$

From Eqs. (34) and (35), the spectral function $A(\mathbf{k},\omega)$ is obtained by using

$$A(\mathbf{k},\omega) = -\operatorname{Im} G(\mathbf{k},\omega). \quad (36)$$

The density of states (DOS) is given by

$$N(\omega) = \int_{-\pi}^{\pi}\int_{-\pi}^{\pi} A(\mathbf{k},\omega) dk_x dk_y, \quad (37)$$

and, finally, the hole density (δ) is obtained by integrating the DOS over the occupied energy states

$$\delta = \int_{-\infty}^{\mu} N(\omega) d\omega. \quad (38)$$

III. RESULTS AND DISCUSSION

We have performed calculations for the hole density, spectral function, and the imaginary part of the self-energy by taking $t_\parallel = 0.4\,\text{eV}$ $t' = 0.25t_\parallel$ and $J_\parallel = 0.3t_\parallel$. Next we define

$$J_\perp = J_\parallel / r, \quad (39)$$

and

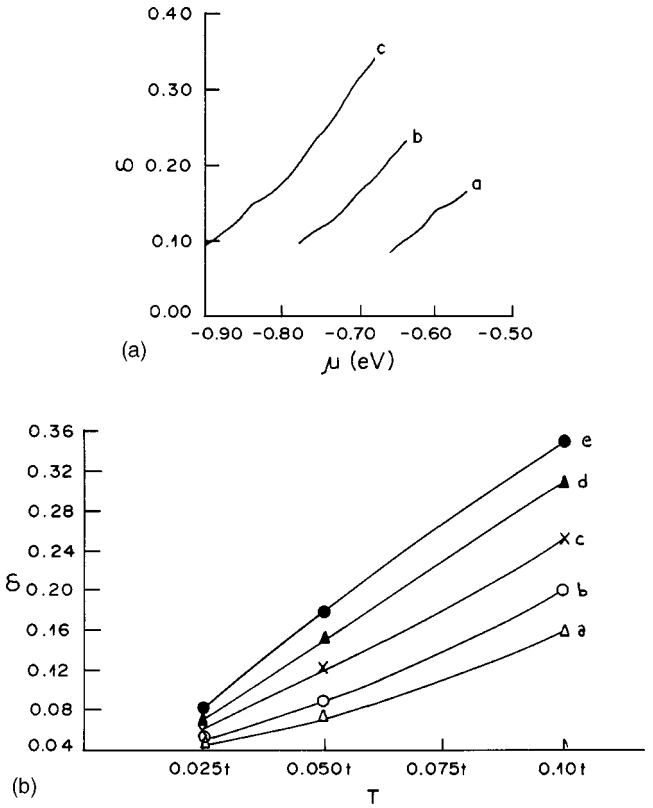

FIG. 2. (a) Variation of hole density (δ) with chemical potential (μ) at (a) $T = 0.025t_\parallel$, (b) $T = 0.05t_\parallel$, and (c) $T = 0.10t_\parallel$ for $r = 10.00$. (b) Variation of hole density (δ) with temperature (T) for various values of chemical potential (μ) for $r = 10.0$. (a) $\mu = -0.82$, (b) $\mu = -0.78$, (c) $\mu = -0.74$, (d) $\mu = -0.70$, and (e) $\mu = -0.68$.

$$t_\perp = t_\parallel / \sqrt{r}. \quad (40)$$

We have scaled $t_\perp$ with $1/\sqrt{r}$ because according to the t-J model, $J = 4r^2/U$ so that for a given onsite Coulomb interaction U, the hopping parameter $t(= t_\parallel, J_\perp)$ is proportional to $\sqrt{J}$ where $J = J_\parallel, J_\perp$. The parameter r signifies the anisotropy of the layered cuprate systems. We have performed calculations for $r = 6.7$ and 10.0. We find that below $r = 6.7$, calculations converge very slowly.

First of all we present results of our calculations for the variation of the hole density (δ) with chemical potential (μ). These results are shown in Fig. 2(a) for $r = 10.0$ and for the temperatures $T = 0.025t_\parallel$, $0.05t_\parallel$, and $0.10t_\parallel$. We find that the present results correspond to a narrow range of μ values as compared to the results of Jaklic and Prelovsek[22] performed for single-layer compounds by using the finite-temperature Lanczos method. Our results can be compared with the right side of the curves of Fig. 1(b) of Ref. 22. In this region, we find a good agreement of our calculated δ versus μ curves with those of Ref. 22.

We next present the results for the hole density as a function of temperature for different values of the chemical potential in Fig. 2(b). From this figure one can infer that for a fixed value of μ, δ increases with increasing temperature. However, for lower values of μ, the rate of increase of the

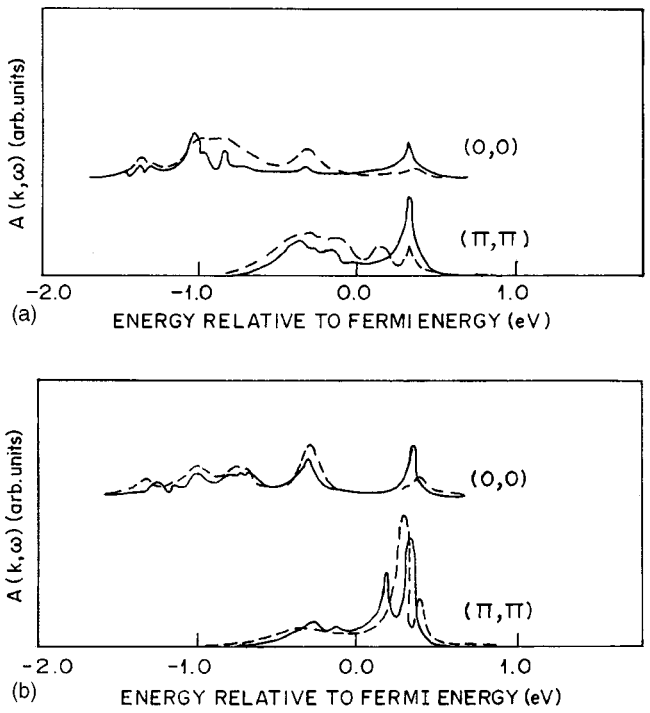

FIG. 3. (a) Doping dependence of spectral function $A(\mathbf{k},\omega)$ at (0,0) and (π,π) points of the Brillioun zone for $r=10.0$ at $T=0.05t_{\|}$, $\delta=0.09$ (dashed line), and $\delta=0.15$ (full line). (b) Temperature dependence of spectral function $A(\mathbf{k},\omega)$ at (0,0) and (π,π) points of the Brillioun zone for $r=10.0$ at $\delta=0.09$. $T=0.025t_{\|}$ (dashed line) and $T=0.10t_{\|}$ (full line).

hole concentration with temperature is less. This T dependence of δ for various values of μ is qualitatively different from that of Jaklic and Perlovsek.[22] In the present case the curves for different values of μ are crowded toward lower values of T, while, in the calculations of Ref. 22, they are crowded toward the higher T. A possible reason for this different behavior may be the bilayer coupling considered in our formalism but not considered by Jaklic and Perlovsek. Other possible reasons may be due to the finite size of the system considered in Ref. 22 and the use of different methodologies in calculating various properties. However, it is not possible to ascertain the relative importance of these factors resulting in a different δ versus T behavior.

We now turn to the presentation of our results for the spectral function $A(\mathbf{k},\omega)$ at different points of the Brillioun zone. Before doing so, we note the form of the intrabilayer hopping parameter $t_{\perp}(\mathbf{k})$ [Eq. (12)]. According to Eq. (12), the intrabilayer hopping has no effect along the $k_x=k_y$ line. Thus the results corresponding to the Brillioun-zone points (0,0), $(\pi/2,\pi/2)$, and (π,π) do not include any effect of the bilayer coupling. The calculated behavior of the spectral function for (0,0) and (π,π) is shown in Fig. 3 for different values of δ and T with $r=10.0$. These results clearly indicate that an increase either in the hole concentration [Fig. 3(a)] or in the temperature [Fig. 3(b)] leads to the appearance of an electronlike quasiparticle character above the Fermi energy. These features are very much similar to those observed in single-layer cuprates.[5,10]

According to Eq. (12), the point $(\pi,0)$ corresponds to the

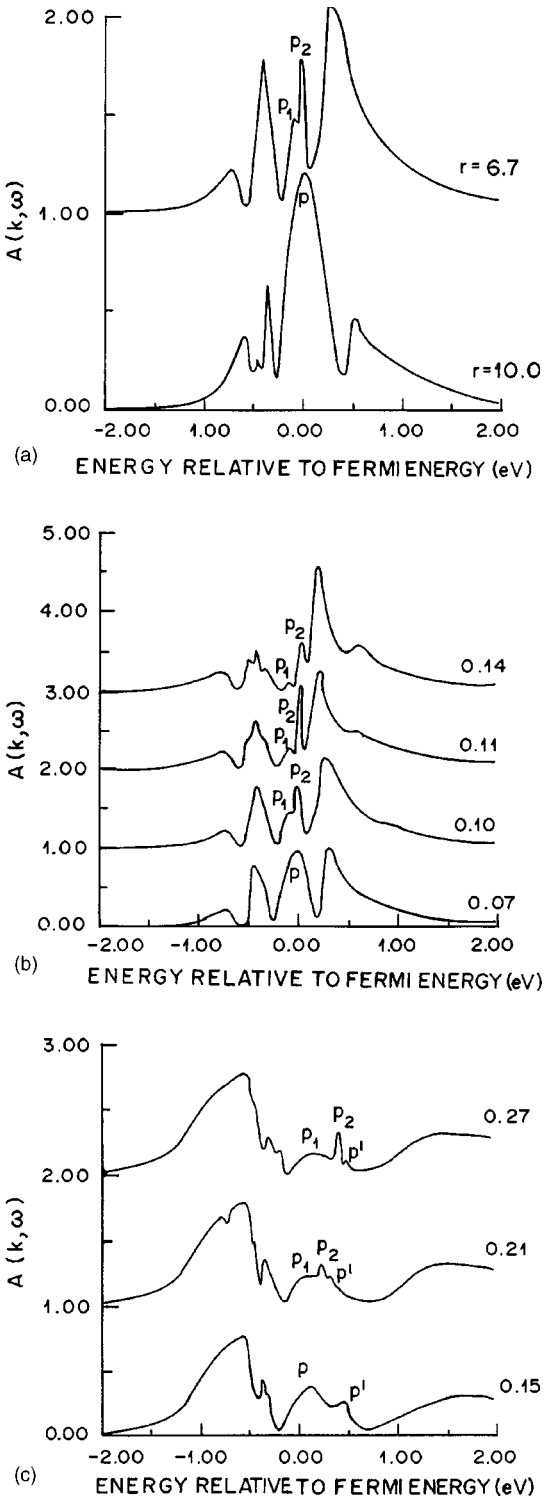

FIG. 4. (a) Effects of anisotropy ratio $\mathbf{r}$ on the spectral function $A(\mathbf{k},\omega)$ at momentum $(\pi,0)$ for $T=0.025t_{\|}$ and $\delta=0.10$. (b) Dependence of $A(\mathbf{k},\omega)$ on δ for $T=0.025t_{\|}$ and $r=6.7$ at momentum $(\pi,0)$. The values next to the curves are the corresponding hole concentration. p marks the broad quasiparticle peak, while p_1 and p_2 represent the two split parts of the peak. (c) Doping dependence of $A(\mathbf{k},\omega)$ at momentum $(\pi,0)$ for $T=0.15t_{\|}$ and $r=10.0$. The value next to the curve is the corresponding hole concentration. p marks the broad quasiparticle peak, while p_1 and p_2 represent the two split parts of the peak.

maximum effect of the coupling of the two layers in the same unit cell. The behavior of $A(\mathbf{k},\omega)$ at $(\pi,0)$ is shown in Fig. 4 for different sets of δ, T, and r values. In Fig. 4(a) we show the behavior of $A(\mathbf{k},\omega)$ at the $(\pi,0)$ point of Brillioun zone for $T=0.025t_{\|}$ and $\delta=0.10$ corresponding to the anisotropy ratio $r=6.7$ and 10.0. It is clear from the figure that for higher anisotropy ($r=10.0$) there is a broad quasiparticle peak (marked as p) in the spectrum. On lowering the anisotropy, this quasiparticle peak splits into two peaks (marked p_1 and p_2). In order to clarify the role of anisotropy we turn to Eq. (40), according to which $r=t_{\|}^2/t_{\perp}^2$. Since in our calculations we have fixed the value of $t_{\|}$, a low value of r implies high value of $t_{\perp}$. Thus, in comparison to $r=10.0$ for $r=6.7$ the value of $t_{\perp}$ increased by a factor of 2.25. With such an enhanced value of $t_{\perp}$, the bilayer effects are much stronger to produce a splitting in the electronic state.

In Fig. 4(b) we analyze the effects of doping on the spectral function at $(\pi,0)$ for $T=0.025t_{\|}$ and $r=6.7$. We observe that the broad peak present at $\delta=0.07$ splits into two peaks (p_1 and p_2) for $\delta>0.10$. In addition, the p_1 peak becomes more and more separated from p_2 upon increasing the doping. The reason for peak splitting with increasing doping lies in the fact that on increasing the doping the coupling between the two CuO_2 layers is effectively enhanced. In fact, this is a peculiar feature of the t-J model where t scales with δ.[4]

We next consider the variation of $A(\mathbf{k},\omega)$ with temperature. In Fig. 4(a) we have already shown that no peak splitting is observed for $T=0.025t_{\|}$ and $r=10.0$. However, since with increased temperature the higher-energy states will also be occupied, which will effectively enhance the bilayer coupling, we expect peak splitting for higher values of T in our calculations. In order to examine this expected result, we have carried out the calculations at elevated temperatures for $r=10.0$. These results are shown in Fig. 4(c). We find that at high T and high δ values the peak in fact splits even for $r=10.0$. In Fig. 4(c) one sees a peak marked p' which may be mistaken for a split peak. However, we mention that p' is a separate peak which exists for all δ values (0.15, 0.21, and 0.27). The peak p which is a single peak for $\delta=0.15$ is split into two peaks p_1 and p_2 for $\delta=0.21$ and $\delta=0.27$.

These features of spectral function at $(\pi,0)$ point, as obtained in Figs. 4(a) and 4(b) are consistent with recent ARPES measurements performed on the underdoped as well as the overdoped bilayer system $Bi_2Sr_2CaCu_2O_{8+y}$.[8,9,11] Our results of Fig. 4(c) are yet to be tested, as there exists no experimental observation of spectral function at high temperatures.

We now focus our attention to evaluate the imaginary part of the self-energy $[\Sigma_1''(\mathbf{k},\omega)]$ for $(k_x,k_y)=(0,0)$, $(\pi/2,\pi/2)$ and $(\pi,0)$ points of the Brillioun zone. The result is presented in Fig. 5 for $\delta=0.15$, $r=10.0$, and $T=0.025t_{\|}$. From this figure it is clear that $\Sigma_1''(\mathbf{k},\omega)$ shows a strong dependence on the momentum $\mathbf{k}$. A strong $\mathbf{k}$ dependence of $\Sigma_1''(\mathbf{k},\omega)$ is also obtained in the other theoretical calculations.[24] Because of this strong $\mathbf{k}$ dependence of $\Sigma_1''(\mathbf{k},\omega)$, care should be taken in describing the excitations of the system. In particular, it would be inappropriate to use a marginal Fermi-liquid description[30] which ignores the $\mathbf{k}$ dependence of $\Sigma_1''(\mathbf{k},\omega)$. In fact, a description of excitations in terms of Anderson-Luttinger liquid theory,[31] which considers the self-energy to be $\mathbf{k}$ dependent, seems to be more reasonable.

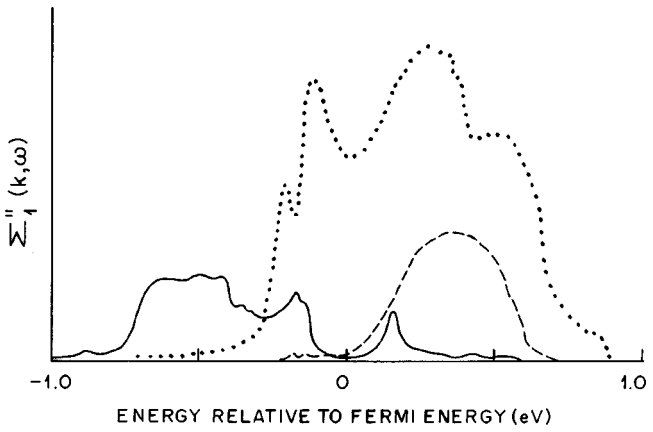

FIG. 5. Imaginary part of the self-energy at $T=0.025t_{\|}$. $\delta=0.15$, and $r=10.0$ for $(k_x,k_y)=(0,0)$ (full line). $(\pi/2,\pi/2)$ (dashed line), and $(\pi,0)$ (dotted line).

The imaginary part of the self-energy shows a very complicated behavior with respect to the energy ω. We observe that near $\omega=0$, $\Sigma_1''(\mathbf{k},\omega)$ follows a ω^2 behavior for $(k_x,k_y)=(0,0)$. This indicates that near this point the system may be described by a Fermi-liquid behavior. On the other hand, for $(\pi/2,\pi/2)$ and $(\pi,0)\Sigma_1''(\mathbf{k},\omega)$ follows a power-law behavior ($\omega^{\alpha},\alpha<2$) near $\omega=0$. Several experiments have shown the power-law behavior of $\Sigma_1''(\mathbf{k},\omega)$ at low ω.[32–34] In addition, some theories also yield a power-law variation of $\Sigma_1''(\mathbf{k},\omega)$ provided $\hbar/\Sigma_1''(\mathbf{k},\omega)$ has the significance of a hole lifetime.[31,35–37] These theories provide quite different origins of the ω^{α}- like dependence of $\Sigma_1''(\mathbf{k},\omega)$. For instance, Anderson[31] suggested the origin of the power-law behavior of $\Sigma_1''(\mathbf{k},\omega)$ to be due to the cuprate systems being two-dimensional Luttinger liquids. On the other hand, Stojkovic and Pines[35] obtained a ω^{α}-like dependence of $\Sigma_1''(\mathbf{k},\omega)$ on the basis of spin fluctuations under the conditions of various nesting effects of the Fermi surface. Finally, ω^{α}-like behavior was also obtained by considering the combined effects of the Coulomb interaction and the electron-phonon interaction.[36,37]

IV. CONCLUSIONS

In conclusion, we have performed a detailed study of the spectral function of bilayer cuprates over a wide range of momentum, hole concentration, temperature, and anisotropy ratio. We note from the present study of $A(\mathbf{k},\omega)$ that the bilayer coupling significantly affects the behavior of hole dynamics in the system. In particular, we obtain a splitting of the electronic states for overdoped systems. The spectral functions $A(\mathbf{k},\omega)$ are asymmetric with respect to the Fermi energy, and, on increasing the hole density, at $k=(0,0)$ and (π,π) points an electronlike quasiparticle character appears in the spectrum. The essential difference from the single-layer compounds is observed at $(\pi,0)$ point of the Brillioun

zone. At $(\pi,0)$ we observe a clear splitting of the peak. The peak splitting is found to be dependent on the anisotropy ratio, the hole density, and the temperature of the system. On the basis of our theoretical results, we have described various situations for bilayer cuprates ranging from underdoped to overdoped regimes under which the peak splitting becomes observable. We have also studied the imaginary part of the self-energy, which is found to be highly **k** dependent, and which does not agree with the marginal Fermi-liquid theory.

ACKNOWLEDGMENTS

This work was financially supported by the Department of Science & Technology (DST), Government of India via Grant No. SP/S2/M-32/99. One of us (Govind) is thankful to the Council for Scientific and Industrial Research (CSIR), Government of India, for financial support via Grant No. 31/1/(180)/2000EMR-I.

[1] W. E. Pickett, Rev. Mod. Phys. **61**, 433 (1989).
[2] F. C. Zhang and T. M. Rice, Phys. Rev. B **37**, 3759 (1988).
[3] B. Keimer, N. Belk, R. J. Birgeneau, A. Cassanho, C. Y. Chen, M. Greven, M. A. Kastner, A. Aharnoy, Y. Endoh, R. W. Erwin, and G. Shirane, Phys. Rev. B **46**, 14 034 (1992); Y. Koike, Y. Iwabuchi, S. Hosoya, N. Kobayashi, and T. Fukase, Physica C **159**, 105 (1989).
[4] E. Dagotto, Rev. Mod. Phys. **66**, 763 (1994).
[5] T. Tohyama and S. Maekawa, Supercond. Sci. Technol. **13**, R17 (2000).
[6] C. G. Olson, R. Liu, D. W. Lynch, R. S. List, A. J. Arko, B. W. Veal, Y. C. Chang, P. Z. Jiang, and A. P. Paulikas, Solid State Commun. **76**, 411 (1990).
[7] D. S. Dessau, B. O. Wells, Z. X. Shen, W. E. Spicer, A. J. Arko, R. S. List, D. B. Mitzi, and A. Kapitulnik, Phys. Rev. Lett. **66**, 2160 (1991).
[8] D. L. Feng, N. P. Armitage, D. H. Liu, A. Damascelli, J. P. Hu, P. Bogdanov, A. Lanzara, F. Ronning, K. M. Shen, H. Eisaki, C. Kim, and Z. X. Shen, cond-mat/0102385 (unpublished).
[9] Y.-D. Chuang, A. D. Gromko, A. Fedorov, D. S. Dessau, Y. Aiura, K. Oka, Y. Ando, H. Eisaki, and S. I. Uchida, cond-mat/0102386 (unpublished).
[10] Z. X. Shen and D. S. Dessau, Phys. Rep. **253**, 1 (1995).
[11] J. Mesot, M. Boehm, M. R. Norman, M. Randeria, N. Metoki, A. Kaminski, S. Rosenkranz, A. Hiess, H. M. Fretwell, J. C. Campuzano, and K. Kadowaki, cond-mat/0102339 (unpublished).
[12] C. L. Kane, P. A. Lee, and N. Read, Phys. Rev. B **39**, 6880 (1989).
[13] E. Dagotto, R. Joynt, A. Moreo, S. Bacci, and E. Gagliano, Phys. Rev. B **41**, 9049 (1990).
[14] D. Poilblanc, T. Ziman, H. J. Schulz, and E. Dagotto, Phys. Rev. B **47**, 14 267 (1993).
[15] A. Moreo, S. Hass, A. W. Sandvik, and E. Dagotto, Phys. Rev. B **51**, 12 045 (1995).
[16] M. Boninsegni and E. Manousakis, Phys. Rev. B **47**, 11 897 (1993).
[17] N. Bulut, D. J. Scalpapino, and S. R. White, Phys. Rev. B **50**, 7215 (1994).
[18] R. Preuss, W. Hanke, C. Grober, and H. G. Evertz, Phys. Rev. Lett. **79**, 1122 (1997).
[19] For details, see E. Dagotto, Rev. Mod. Phys. **66**, 763 (1994).
[20] S. R. White, Phys. Rev. Lett. **69**, 2863 (1992).
[21] X. Wang and T. Xiang, Phys. Rev. B **56**, 5061 (1997).
[22] J. Jaklic and P. Prelovsek, Phys. Rev. Lett. **77**, 892 (1996).
[23] J. Jaklic and P. Prelovsek, Phys. Rev. B **55**, R7307 (1997).
[24] For details on numerical studies, see J. Jacklic and P. Prelovsek, Adv. Phys. **49**, 1 (2000).
[25] S. Chakarvarty, A. Sudbo, P. W. Anderson, and S. Strong, Science **261**, 337 (1993).
[26] A. I. Liechtenstein, O. Gunnarsson, O. K. Anderson, and R. M. Martin, Phys. Rev. B **54**, 12 505 (1996); O. K. Anderson, A. I. Liechtenstein, O. Jepsen, and F. Paulsen, J. Phys. Chem. Solids **56**, 1573 (1995).
[27] A. Pratap, Govind, and R. S. Tripathi, Phys. Rev. B **60**, 6775 (1999), and references therein.
[28] P. Dai, H. A. Mook, S. M. Hayden, G. Aeppli, T. G. Perring, R. D. Hunt, and F. Dogan, Science **284**, 1344 (1999).
[29] J. L. Richard and V. Yu. Yushankhai, Phys. Rev. B **47**, 1103 (1993); J. L. Richard and V. Yu. Yushankhai, Phys. Rev. B **50**, 12 927 (1994).
[30] C. M. Varma, P. B. Littlewood, S. Schmitt-Rink, E. Abrahams, and A. E. Ruckenstein, Phys. Rev. Lett. **26**, 1996 (1989).
[31] P. W. Anderson, *The Theory of Superconductivity in High-T_C Cuprates* (Princeton University Press, Princeton, 1997).
[32] Z. Schlesinger, R. T. Collins, F. Holtzberz, C. Field, S. H. Blanton, U. Welp, G. W. Crabtree, Y. Fang, and J. Z. Liu, Phys. Rev. Lett. **65**, 801 (1990).
[33] S. Uchida, Physica C **185-189**, 28 (1991).
[34] A. V. Puchkov, D. N. Basov, and T. Timusk, J. Phys.: Condens. Matter **8**, 10 049 (1996), and references therein.
[35] B. P. Stojkovic and D. Pines, Phys. Rev. B **56**, 11 931 (1997).
[36] Ratan Lal, Solid State Commun. **115**, 359 (2000).
[37] Ratan Lal, Physica C **71**, 340 (2000).